Spin-Flip Limited Exciton Dephasing in CdSe/ZnS Colloidal Quantum Dots

Francesco Masia, Nicolò Accanto, Wolfgang Langbein, and Paola Borri

Cardiff University School of Physics and Astronomy and School of Biosciences, The Parade, Cardiff CF24 3AA, United Kingdom

(Received 27 July 2011; published 22 February 2012)

The dephasing time of the lowest bright exciton in CdSe/ZnS wurtzite quantum dots is measured from 5 to 170 K and compared with density dynamics within the exciton fine structure using a sensitive three-beam four-wave-mixing technique unaffected by spectral diffusion. Pure dephasing via acoustic phonons dominates the initial dynamics, followed by an exponential zero-phonon line dephasing of 109 ps at 5 K, much faster than the ~10 ns exciton radiative lifetime. The zero-phonon line dephasing is explained by phonon-assisted spin flip from the lowest bright state to dark-exciton states. This is confirmed by the temperature dependence of the exciton lifetime and by direct measurements of the bright-dark–exciton relaxation. Our results give an unambiguous evidence of the physical origin of the exciton dephasing in these nanocrystals.

DOI: 10.1103/PhysRevLett.108.087401 PACS numbers: 78.67.Hc, 42.50.Md, 63.22.−m, 78.47.nj

The optical properties of excitons in colloidal semiconductor quantum dots (CQDs) of size comparable or smaller than the exciton Bohr radius have been the subject of intensive research for many years, also owing to the simplicity of colloidal synthesis and the consequent easiness to practically engineer CQD size, shape, composition, and in turn quantum confinement [1]. One of the greatest hopes with these nanostructures is to achieve atomlike absorption and emission spectra and in turn ultralong exciton coherence, attractive for applications ranging from cavity quantum electrodynamics [2] to laser technology [3]. Among the various material types, CdSe CQDs were studied since early days [1]. Noticeably, their strong and spectrally wide absorption, combined with a narrow and size-tuneable emission spectrum in the visible range, has promoted their application as biolabels [4] and in photovoltaics, invigorating the interest in CQDs.

The excitonic level structure in CdSe CQDs has been treated theoretically [5] and is nontrivial. Because of the s-like conduction band, p-like valence band, and the electron and hole spin, the envelope ground state contains 12 sublevels. Spin-orbit coupling splits the p-like valence band according to the hole total angular momentum J into the $J = 3/2$ and $J = 1/2$ bands, the latter being at lower energies and thus not further considered. The $J = 3/2$ band itself is split by the hexagonal crystal structure according to the angular momentum projection M along the crystal c axis, into the heavy-hole $|M| = 3/2$ and the light-hole $|M| = 1/2$ (crystal-field splitting). The resulting levels are split further by shape asymmetry and electron-hole exchange interaction [5]. Assuming a shape which retains cylindrical symmetry around c, exciton levels are classified by the absolute value of the total angular momentum projection $|F|$ along c. For large sizes and small or oblate ellipticity, the lowest exciton level is of heavy-hole character, twofold degenerate and dark with $|F| = 2$, and lies a few meV below a twofold degenerate bright level with $|F| = 1$. Prolate (i.e., rod-shaped) shape asymmetry counteracts the crystal-field splitting in CdSe, eventually pushing the light-hole states below the heavy-hole states and resulting in a lower dark $F = 0$ state, called 0^L, becoming the lowest level below the bright $|F| = 1$ level [5,6].

The dephasing time and in turn the homogeneous linewidth of the lowest bright ground-state exciton level in wurtzite CdSe CQDs was first addressed experimentally by Schoenlein *et al.* [7,8] in 2–4 nm diameter nanocrystals using transient three-beam four-wave mixing (FWM) photon echo. Within the available dynamic range, an ultrafast dephasing of 85–270 fs was found at low temperature and attributed to acoustic phonon interactions. Subsequent spectral-hole burning experiments [9] on larger CdSe/ZnS core/shell CQDs with 9 nm core diameter demonstrated a composite homogeneous line shape with a sharp zero-phonon line (ZPL) of 6 μeV linewidth full width at half maximum (FWHM) at 2 K, corresponding to 200 ps dephasing time, superimposed on a few-meV broadband due to phonon-assisted transitions. Such a composite line shape and a ZPL of ~10 μeV at low temperature were confirmed by more recent studies on single CdSe/ZnS CQDs [10–12]. On the other hand, the radiative lifetime of the lowest bright ground-state exciton is ~10 ns [13], indicating that even a 200 ps dephasing time is not radiatively limited. Single-dot photoluminescence (PL) as well as spectral-hole burning experiments are affected by spectral diffusion, a variation of the CQD transition frequency over time from slow fluctuations of the CQD environment. It was thus speculated in those reports that the measured ~10 μeV linewidth was limited by spectral diffusion and that a coherence lifetime of ~100 ps was only a lower bound.

We previously demonstrated in self-assembled quantum dots that transient resonant FWM overcomes not only the inhomogeneous broadening in ensembles via the

photon-echo formation but also spectral diffusion [14]. By combining directional selection with heterodyne detection, we achieved shot-noise limited detection sensitivity and a large dynamic range [15]. In this Letter, we have applied this technique to CdSe/ZnS CQD ensembles and, owing to its much greater dynamic range compared to Ref. [7], resolved the ZPL dephasing of the lowest bright ground-state exciton level, not limited by spectral diffusion.

We investigated high-quality wurtzite CdSe/ZnS CQDs (Qdot655, Invitrogen), nominally identical to those used in Refs. [10,11], with a room-temperature PL peak emission wavelength at 655 nm [see Fig. 1(a)] and an average core size of 8 nm. High-resolution transmission electron microscopy shows that the dots are typically nonspherical with a rod-shaped core of ~5 nm diameter and ~10 nm length. The CQDs were dispersed in a polystyrene film and sandwiched between two quartz windows mounted onto a cold-finger cryostat. To preferentially excite the lowest bright ground-state excitonic absorption, the center wavelength of the exciting pulses was tuned below the PL emission at low temperature by an amount of the order of the Stokes shift (~ 40 meV) in these CQDs. We used a three-beam geometry, as sketched in Fig. 1(b), where each beam is a train of 150 fs pulses with 76 MHz repetition rate. The first pulse (P_1) induces a coherent polarization in the sample, which after a delay τ_{12} is converted into a density grating by the second pulse (P_2). The third pulse (P_3), delayed by τ_{23} from P_2, is diffracted and frequency-shifted by this density grating which is moving in the heterodyne technique [15], providing the FWM field, which is detected by its interference with a reference pulse of adjustable delay. In an inhomogeneously broadened ensemble, the FWM signal is a photon echo emitted at τ_{12} after P_3 and the microscopic dephasing is inferred from the decay of the photon-echo amplitude versus τ_{12}. Conversely, the decay of the photon-echo amplitude versus τ_{23} probes the exciton density dynamics [16]. We recently applied this technique to compare the dephasing time and exciton density dynamics in PbS CQDs [17]. To minimize selective excitation of linearly polarized transitions in the ensemble of randomly oriented CQDs, all pulses were cocircularly polarized.

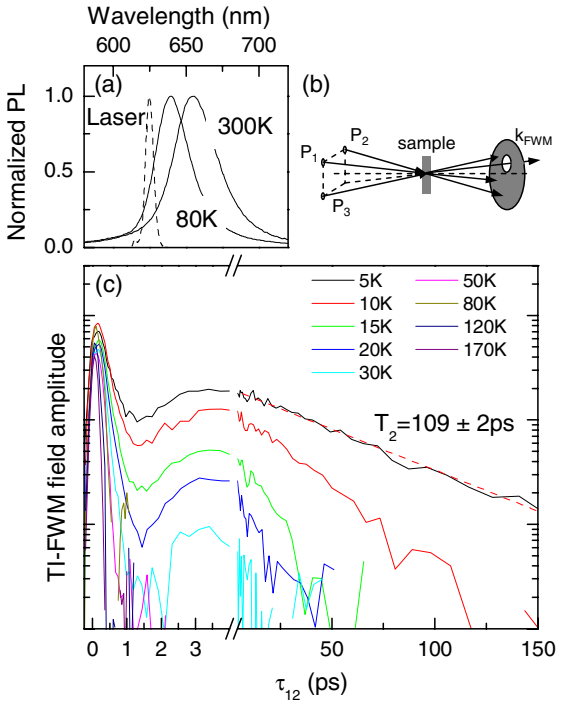

FIG. 1 (color online). (a) Normalized PL spectra (solid lines) of the investigated CdSe/ZnS wurtzite CQDs. The dashed line shows the pulse laser spectrum used in the transient FWM experiment. (b) Sketch of the three-beam FWM directional geometry. (c) Time-integrated FWM field amplitude measured at different temperatures versus delay between the first two pulses. The dashed line is a single exponential fit to the data at 5 K.

The time-integrated FWM (TI-FWM) field amplitude is shown in Fig. 1(c) as a function of τ_{12} for different temperatures. Measurements are taken for nonzero $\tau_{23} = 1$ ps to avoid nonresonant nonlinearities. The time-averaged excitation intensity of ~60 W/cm^2 per beam was well within the third-order nonlinear regime and also resulted in negligible local heating, as we affirmed by power-dependent measurements. Remarkably, the dephasing is initially very fast even at 5 K, but, within the dynamic range of 3 orders in FWM field corresponding to *6 orders in FWM intensity*, a long monoexponential dephasing time (T_2) is resolved at larger τ_{12}. With increasing temperature, the initial dephasing becomes faster and more dominant, while simultaneously T_2 decreases. This behavior reflects in the time domain the composite homogeneous line shape consisting of a sharp Lorentzian ZPL (corresponding to the long exponential dephasing) superimposed onto a broad acoustic phonon band (the initial fast dephasing), also observed in self-assembled quantum dots [18]. It is due to the excitation of localized carriers, which distorts the lattice equilibrium and thus couples the optical transition with phonon absorption and emission processes similar to rotovibrational bands in molecules. With increasing temperature, it is expected that the weight of the ZPL (defined as the area fraction of the ZPL in the linear absorption spectrum) decreases and the width of the phonon band increases [18].

From the dynamics in Fig. 1, we have quantified in Fig. 2(a) the temperature dependence of the ZPL width $\gamma_{\mathrm{ZPL}} = 2\hbar/T_2$, the FWHM of the acoustic phonon band Γ_{ph}, and the ZPL weight Z, using the method discussed in Ref. [18]. Γ_{ph} is obtained by an exponential fit to the initial FWM decay, which is an approximation since the phonon broadband is non-Lorentzian but is in qualitative agreement with what was obtained by Fourier transforming the FWM dynamics [14]. Above 80 K, the initial dephasing becomes faster than the pulse duration in the experiment;

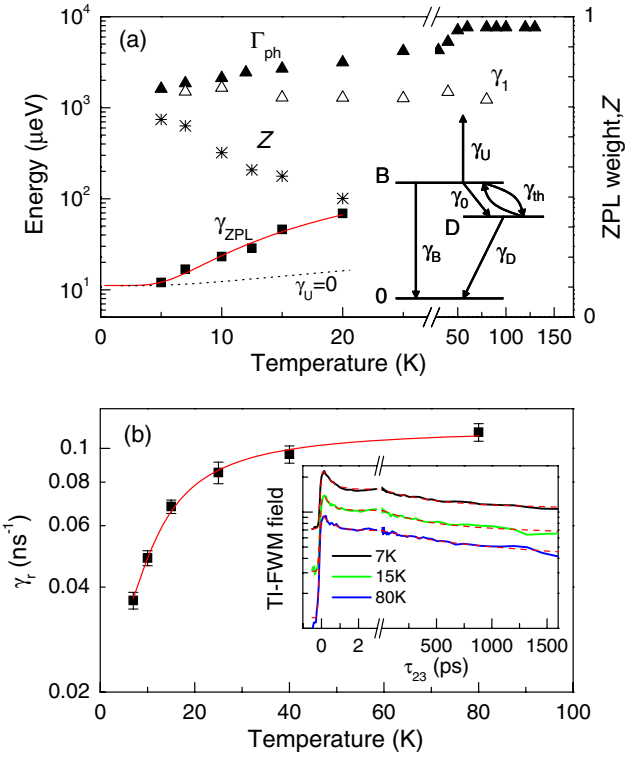

FIG. 2 (color online). (a) Homogenous linewidth FWHM of the ZPL (γ_{ZPL}, squares) and of the acoustic phonon band (Γ_{ph}, triangles) versus temperature in CdSe/ZnS wurtzite CQDs. The ZPL weight Z is also shown (stars). The inset is a sketch of the lower bright-dark–exciton relaxation model. The solid line onto γ_{ZPL} is a fit to the data (see text). The dotted line is a fit without the absorption rate. (b) Long-lived exciton lifetime versus temperature as measured from the exciton density dynamics (see inset) by TI-FWM versus τ_{23} at $\tau_{12} = 0$. The solid line is a fit to the data. Dashed lines in the inset are multiexponential fits to the dynamics. γ_1 in (a) is the broadening estimated from the initial subpicosecond density dynamics (see text).

hence, the reported Γ_{ph} represents a lower bound. Besides the expected behavior of Z and the acoustic phonon band, we observe a decrease of γ_{ZPL} with decreasing temperature. Importantly, the measured $T_2 = 109 \pm 2$ ps ($\gamma_{ZPL} = 12$ μeV) at 5 K not limited by spectral diffusion clearly shows that the ZPL dephasing is far from the $\sim$10 ns radiative limit, which raises the question of its physical origin.

It was shown in Ref. [13] by temperature-dependent time-resolved PL in single-wurtzite CdSe/ZnS CQDs that rapid thermalization occurs between the lowest bright and the lowest dark levels, following a three-level model, as sketched in the inset of Fig. 2(a). Within this model, after photoexcitation into the bright state (B), rapid phonon-assisted relaxation occurs into the dark state (D), with a low-temperature spin-flip rate $\gamma_0 \sim 10$ ns^{-1}, which is much larger than the radiative recombination rate of the bright state $\gamma_B \sim 0.1$ ns^{-1}. With increasing temperature, not only spontaneous emission but also stimulated emission and absorption of acoustic phonons with energy equal to the bright-dark splitting ΔE_D occur with a rate $\gamma_{th} = \gamma_0 N_B$, where $N_B = 1/[\exp(\Delta E_D/k_B T) - 1]$ is the phonon occupation number. For $k_B T \ll \Delta E_D$, radiative recombination takes place mainly from the dark state with a long lifetime $(\gamma_D)^{-1} \sim 1$ μs [13]. For $k_B T \gg \Delta E_D$, thermalization between bright and dark states results in a higher occupation probability of the bright state. Exciton recombination therefore occurs from both levels, and the total decay rate is the thermal average between the two rates. Since $\gamma_0 \gg \gamma_B$, such a spin flip could be the origin of the nonradiatively limited γ_{ZPL}.

To prove this mechanism in our sample, we have first investigated the temperature dependence of the exciton decay rate by measuring FWM versus τ_{23} [see Fig. 2(b)]. The probed exciton density exhibits a multiexponential decay which we fit with three time constants in the subpicosecond, hundreds of picoseconds, and few-nanosecond ranges [see the inset of Fig. 2(b)]. The first subpicosecond time constant is attributed to a subensemble of CQDs resonantly excited in the upper bright states, showing a rapid relaxation towards the lower states. This time constant is not temperature-dependent up to 80 K, consistently with $\sim$20 meV crystal-field splitting [5] and correspondingly negligible phonon occupation up to 80 K. Such a finding, however, implies that the initial dephasing in Fig. 1(c) might include this relaxation. To quantify this effect, we have plotted in Fig. 2(a) the homogeneous broadening γ_1 resulting from the sub-ps relaxation from the upper bright states. We find that $\Gamma_{ph} > \gamma_1$ above 7 K, indicating that the initial dephasing is dominated by the acoustic phonon broadband at these temperatures. However, at 5 K, due to this contribution, we could be underestimating the ZPL weight by about 10% (as deduced from the $\sim$30% amplitude drop of the sub-ps density dynamics and the cubic relationship between the FWM field and Z [18]). The second time constant of $\sim$400 ps found in the density dynamics is temperature-independent and attributed to the Auger recombination of charged excitons. The longest time constant, manifesting as a pulse-to-pulse pileup included in our fit, corresponds to a recombination rate γ_r which increases with increasing temperature [see Fig. 2(b)], consistent with Ref. [13].

The three-level model sketched in the inset of Fig. 2(a) explains the temperature dependence of both γ_{ZPL} and γ_r. In this model, the dephasing rate is given by $\gamma_{ZPL} = \gamma_B + \gamma_0 + \gamma_{th} + \gamma_U$, where γ_B is the radiatively limited dephasing of the bright state, $\gamma_0 + \gamma_{th}$ is the spin-flip relaxation into the dark state via spontaneous and stimulated phonon emission, and γ_U accounts for phonon absorption into an upper level. γ_r is the thermal average of the radiative rates of the bright, the lower dark, and the upper level, with their occupation probabilities and degeneracy. By performing a combined fit of the measured temperature dependencies of γ_{ZPL} and γ_r, we find that the dephasing rate is dominated

by $\gamma_0 + \gamma_U$ while the stimulated emission term γ_{th} is actually negligible up to 20 K (see the dotted line in Fig. 2) considering the bright-dark splitting $\Delta E_D = 2.0 \pm 0.2$ meV found from the fit of γ_r (see below). From the fit of γ_{ZPL}, we deduce $\gamma_0 = 11 \pm 0.5$ μeV (corresponding to a 17 ns^{-1} spontaneous spin-flip rate) and a phonon absorption γ_U with amplitude 130 ± 40 μeV and activation energy $\Delta E_U = 2.2 \pm 0.3$ meV. In prolate CQDs, theory predicts [5] that the dark level 0^L approaches the lowest bright $|F| = 1$, with a crossover close to the ~5 nm diameter and ~10 nm length [6] mostly found in our sample. We thus tentatively attribute this upper level to the 0^L dark state [19]. The measured temperature dependence of γ_r is well-described by $\gamma_r = [2\gamma_B + 2\gamma_D \exp(\Delta E_D/k_B T) + \gamma_D \exp(-\Delta E_U/k_B T)]/[2 + 2\exp(\Delta E_D/k_B T) + \exp(-\Delta E_U/k_B T)]$, where for simplicity we have assumed the radiative rate of the dark state γ_D to be equal for the lower and upper dark levels. We find that the temperature dependence is dominated by the thermalization into the lowest dark state; hence, the fit to the measured γ_r is mostly sensitive to the lowest bright-dark splitting $\Delta E_D = 2.0 \pm 0.2$ meV, with $\gamma_B = 2.4 \pm 0.1 \times 10^{-1}$ ns^{-1} [20]. Importantly, $\gamma_B \ll \gamma_0$; thus, the zero-temperature extrapolated γ_{ZPL} is indeed γ_0 limited by the spin-flip rate.

To further verify this attribution, we directly determined the bright-dark relaxation by measuring for $\tau_{12} > 0$ the FWM amplitude versus τ_{23}, which is sensitive to the density dynamics within the fine structure since a spectrally modulated density grating is created. Specifically, for the dark-bright relaxation, one can understand this as follows. At $\tau_{12} = 0$, the creation of an exciton by the P_1 and P_2 pulses makes the sample transparent to the probe P_3, since stimulated emission at the ground-state to bright-exciton transition (0-B) and absorption at the bright-exciton to biexciton transition (B-XX) compensate (note that the biexciton binding energy E_{XX} is smaller that the spectral width of the pulses). If the exciton is in the dark state, the sample is also transparent to P_3, since both absorption and stimulated emission are forbidden. We are thus not sensitive to the dark-bright relaxation for $\tau_{12} = 0$. Conversely, for $\tau_{12} > 0$, the phase difference between the fields from the 0-B and B-XX transitions at the photon-echo time is $\pi + E_{XX}\tau_{12}/\hbar$, resulting in exciton-biexciton beats versus τ_{12} [16,21]. We indeed observe weak oscillations in the TI-FWM versus τ_{12} with a modulation period in the 3–6 ps range. In particular, for τ_{12} equal to half the exciton-biexciton beat period, 0-B and B-XX fields interfere constructively, as opposed to the destructive interference at $\tau_{12} = 0$. A spin flip into a dark level instead reduces the field to zero. A bright-dark relaxation thus manifests as a decrease in the FWM signal versus τ_{23}, which is most pronounced for τ_{12} equal to half the exciton-biexciton beat period. In Fig. 3, the measured FWM amplitude versus τ_{23} at 10 K is shown for three different values of τ_{12} and the dashed lines are fits using a biexponential decay, plus an offset accounting for the long radiative lifetime. The biexponential decay consists of a new time constant (τ_s) present only for $\tau_{12} > 0$ and the 400 ps time constant previously discussed. We see that the effect of τ_s is most pronounced for $\tau_{12} = 1.5$ ps and we can consistently fit all dynamics for $\tau_{12} \neq 0$ with $\tau_s = 27 \pm 7$ ps at 10 K. This spin-flip time is in very good agreement with the density lifetime $T_2/2$ deduced from the measured ZPL dephasing, as shown in Fig. 3(b). Similar measurements carried out at 15 K confirm this agreement.

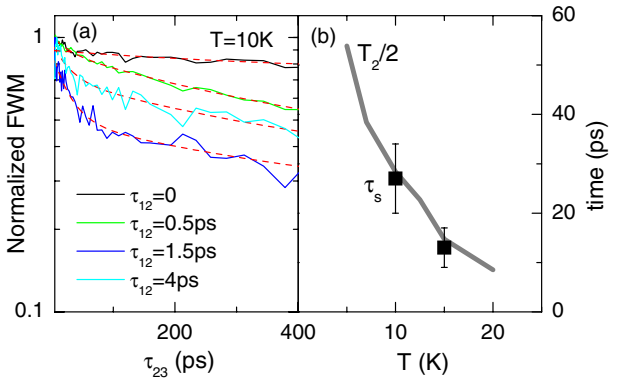

FIG. 3 (color online). (a) TI-FWM field versus τ_{23} for different τ_{12}, together with fits (dashed lines) to the dynamics. (b) The additional time constant τ_s (squares) inferred from the dynamics at $\tau_{12} \neq 0$ is compared with the measured ZPL dephasing time.

In conclusion, we have shown that the intrinsic zero-phonon line dephasing of the ground-state exciton in CdSe/ZnS wurtzite colloidal quantum dots is limited even at low temperatures by the rapid (~ 100 ps) spin flip from the lower bright-to-dark–exciton levels. This finding is different from InGaAs self-assembled quantum dots, where the bright-dark–exciton relaxation is longer than the radiative lifetime and the exciton dephasing is radiatively limited [22]. Our results conclusively resolve the long-standing question of the physical origin of the ZPL broadening in CdSe/ZnS quantum dots.

We acknowledge discussions on the excitonic fine structure with Iwan Moreels at Ghent University (Belgium). F. M. acknowledges the European Union (Marie Curie Grant Agreement No. PIEF-GA-2008-220901) and the Welcome Trust. P. B. received support from the EPSRC U.K. Research Council (Grant No. EP/I005072/1).

[1] A. Alivisatos, Science **271**, 933 (1996).
[2] N. L. Thomas, U. Woggon, O. Schöps, M. V. Artemyev, M. Kazes, and U. Banin, Nano Lett. **6**, 557 (2006).
[3] V. I. Klimov, A. A. Mikhailovsky, S. Xu, A. Malko, J. A. Hollingsworth, C. A. Leatherdale, H.-J. Eisler, and M. G. Bawendi, Science **290**, 314 (2000).
[4] X. Michalet, F. F. Pinaud, L. A. Bentolila, J. M. Tsay, S. Doose, J. J. Li, G. Sundaresan, A. M. Wu, S. S. Gambhir, and S. Weiss, Science **307**, 538 (2005).

[5] A. L. Efros, M. Rosen, M. Kuno, M. Nirmal, D. J. Norris, and M. Bawendi, Phys. Rev. B **54**, 4843 (1996).
[6] Q. Zhao, P. A. Graf, W. B. Jones, A. Franceschetti, J. Li, L.-W. Wang, and K. Kim, Nano Lett. **7**, 3274 (2007).
[7] R. W. Schoenlein, D. M. Mittelman, J. J. Shiang, A. P. Alivisatos, and C. V. Shank, Phys. Rev. Lett. **70**, 1014 (1993).
[8] D. M. Mittleman, R. W. Schoenlein, J. J. Shiang, V. L. Colvin, A. P. Alivisatos, and C. V. Shank, Phys. Rev. B **49**, 14 435 (1994).
[9] P. Palinginis, S. Tavenner, M. Lonergan, and H. Wang, Phys. Rev. B **67**, 201307(R) (2003).
[10] M. J. Fernée, B. N. Littleton, S. Cooper, H. Rubinsztein-Dunlop, D. E. Gómez, and P. Mulvaney, J. Phys. Chem. C **112**, 1878 (2008).
[11] L. Biadala, Y. Louyer, P. Tamarat, and B. Lounis, Phys. Rev. Lett. **103**, 037404 (2009).
[12] L. Coolen, X. Brokmann, P. Spinicelli, and J.-P. Hermier, Phys. Rev. Lett. **100**, 027403 (2008).
[13] O. Labeau, P. Tamarat, and B. Lounis, Phys. Rev. Lett. **90**, 257404 (2003).
[14] P. Borri, W. Langbein, S. Schneider, U. Woggon, R. L. Sellin, D. Ouyang, and D. Bimberg, Phys. Rev. Lett. **87**, 157401 (2001).
[15] P. Borri and W. Langbein, J. Phys. Condens. Matter **19**, 295201 (2007).
[16] J. Shah, *Ultrafast Spectroscopy of Semiconductors and Semiconductor Nanostructures* (Springer, Berlin, 1996), Chap. 2.
[17] F. Masia, W. Langbein, I. Moreels, Z. Hens, and P. Borri, Phys. Rev. B **83**, 201309(R) (2011).
[18] P. Borri, W. Langbein, U. Woggon, V. Stavarache, D. Reuter, and A. D. Wieck, Phys. Rev. B **71**, 115328 (2005).
[19] Near the crossover, it is also possible that the 0^{L} dark state is the lowest dark, and, just above the $|F| = 1$ bright state, there is a dark $|F| = 2$ or a bright 0^{U} state [5,6], the latter possibly contributing to the sub-ps dynamics previously discussed.
[20] A good fit, as shown in Fig. 2(b), is also achieved by considering the lowest level 0^{L} dark and the upper level 0^{U} bright, with $\Delta E_{\mathrm{D}} = 1.7 \pm 0.2$ meV and $\gamma_{\mathrm{B}} = 1.32 \pm 0.03 \times 10^{-1}$ ns^{-1}.
[21] W. Langbein, J. M. Hvam, M. Umlauff, H. Kalt, B. Jobst, and D. Hommel, Phys. Rev. B **55**, R7383 (1997).
[22] W. Langbein, P. Borri, U. Woggon, V. Stavarache, D. Reuter, and A. D. Wieck, Phys. Rev. B **70**, 033301 (2004).